Preparation and Gas Sensing Property of PEDOT/Silica Aerogel Fibers

Si Meng, Xi-yue Huang, Xing-ping Wang, Jun-yan Zhang, Wen-ping Chen and Mei-fang Zhu

Abstract Porous materials, as their high specific surface area, are commonly used in NH_3-sensing. And when NH_3-sensing materials are made into the form with interconnected pore structure, low-dimensional structure or hierarchical structure, their gas-sensitivity will be improved remarkably. Here, firstly silica aerogel fibers were prepared by wet spinning. Those fibers do not only preserve high specific surface area (maximum one is 835.8 m^2/g) and network organization, but also have unique hierarchical structure (macropores in the surface and mesopores in the middle regions) and regular hollow structure. And then PEDOT was synthesized and loaded on the net skeletons of silica aerogel fibers by gas phase polymerization. The specific surface area and pore structure of PEDOT/silica aerogel fibers can be adjusted by change aging bath. Finally, the results of NH_3 sensitivity experiment showed that all fibers have good gas sensitive, especially A0.5-PEDOT/SAFs (resistance variation is over 40%).

Keywords Aerogel fiber · PEDOT · Gas phase polymerization
Gas sensing · Hierarchical

S. Meng · X. Huang · X. Wang · J. Zhang · W. Chen · M. Zhu (✉)
The State Key Laboratory for Modification of Chemical Fibers and Polymer Materials, College of Materials Science and Engineering, Donghua University, Shanghai 201620, China
e-mail: zhumf@dhu.edu.cn

S. Meng
e-mail: mengsi_simon@163.com

X. Huang
e-mail: empt_y@qq.com

X. Wang
e-mail: wxp2100486@sina.com

J. Zhang
e-mail: 13817145747@163.com

W. Chen
e-mail: chwp@dhu.edu.cn

Y. Han (ed.), *Advanced Functional Materials*,
https://doi.org/10.1007/978-981-13-0110-0_83

Introduction

Ammonia sensors are heavily used in agriculture and chemical industry. And the NH_3-sensing material is the core component of ammonia sensors [1, 2]. As NH_3-sensing materials, conductive polymer materials can be used at room temperature or even cooler temperatures, so they are perceived to be more universal than inorganic NH_3-sensing materials [3–6]. However, currently all kinds of conductive polymer NH_3-sensing materials have a much lower sensitivity compared to inorganic one. Therefore, it is the key to make conductive polymer NH_3-sensing materials enter practical and commercialize stage that improving the sensitivity of NH_3-sensing materials [7–10].

PEDOT is a typical conductive polymer materials, and it also has a quite low sensitivity. But compared to other conductive polymer materials, it has higher conductivity and better stability. Those properties have important effect on sensors. In addition, its preparation method is simple. Therefore, PEDOT is one of the hottest topics in sensing materials.

In the field of NH_3-sensing, porous materials often show better sensitivity as their high specific surface area [11, 12]. And when the porous NH_3-sensing materials are made into the form with interconnected pore structure [13, 14], low-dimensional structure [15, 16] or hierarchical structure [17, 18], their gas-sensitivity will be improved remarkably. However, PEDOT with those structures is hardly prepared directly. Therefore, some materials, which have such structures, were chosen as substrate to achieve this. At present, most of substrate materials just have one or two of such structures. Although the sensitivity of PEDOT on those substrate had significantly improvement, it is much lower than the sensitivity of polyaniline, let alone inorganic NH_3-sensing materials [19–21]. If a kind of substrate material with all those structures is prepared to load PEDOT, the sensitivity of PEDOT must be improved further.

Herein, a kind of silica aerogel fibers (SAFs) with high specific surface area, hierarchical structure and hollow structure were prepared as substrate by simple wet spinning. The hollow structure could be beneficial to improve sensitivity [22, 23]. Silica aerogel is a kind of porous material with ultra-high specific surface area and interconnected pore structure. And it is prepared from precursor, for example tetraethyl orthosilioate, sodium silicate and water glass, by sol-gel method. In this work, water glass was selected as precursor and spinning dope, and dilute sulfuric acid was selected as catalyzer, reactant and coagulating bath to prepare silica aerogel precursor fibers (SAPFs) by wet spinning. And then the prepared SAPFs transformed into SAFs by aging and drying. The prepared SAFs do not only preserve high specific surface area and network organization, but also have unique hierarchical structure and regular hollow structure. PEDOT was synthesized and loaded on the net skeletons of silica aerogel fibers by gas phase polymerization, thus PEDOT/SAFs was prepared. Benefited from gas phase polymerization, the gas

phase 3,4-ethoxylene dioxy thiophene (EDOT) can enter the pores of SAFs and form a thin PEDOT film on the skeletons [24–26]. The morphology, structure and sensing performance of SAFs and PEDOT/SAFs were studied. And the pore sizes and specific surface area were adjusted to optimize their sensing performance by change aging bath.

Introduction

Materials. Water glass (Be° = 50, Na_2O:SiO_2 molar ratio = 1:2.2) was purchased from Tongxiang Xiangyang water glass mill, China. Sulfuric acid was purchased from Sinopharm Chemical Reagent Co., Ltd, China. Ethanol was purchased from Changshu Yangyuan Chemical Co., Ltd, China. Iron(III) p-toluene sulfonate hexahydrate and 3,4-ethoxylene dioxy thiophene (EDOT) were purchased from Energy Chemical Co., Ltd, China. Silver paste was purchased from Beijing ZhongJingkeyi Technology Co., Ltd, China. Copper foil was purchased from Dongguan Xinshi Packing Material Co., Ltd, China.

Preparation of SAFs. A typical procedure for preparing SAFs involves three steps, spinning, aging and drying. Initially, 10 ml water glass as spinning dope was filled in an injector. 0.5 mol/L sulfuric acid as coagulating bath was prepared and stored in a polypropylene sink. The needle (inside diameter is 0.4 mm) of the injector connected to another needle (inside diameter is 0.4 mm too) in coagulating bath by a PTFE tube. Water glass was injected into coagulating bath through PTFE tube and needle by injection pump at a rate of 0.1 ml/min. And glass water was translated into solid fibrous orthosilicic acid, namely silica aerogel precursor fibers (SAPFs), rapidly, when it was injected into coagulating bath. The reaction is shown as Eq. 1. The SAPFs was winded continuously by winder at a rate of 80 mm/s. Then the SAPFs were soaked in aging bath for 3 days. The aging bath is different concentration of diluted sulfuric acid solution (0.5, 0.1, 0.05, 0.01 and 0 mol/L, namely pure water). During 3 days aging, the orthosilicic acid fibers would be slowly translated into silica gel fibers by polycondensation, as shown in Eq. 2. Then the solution in silica gel fibers was replaced by ethanol. Finally, the silica gel fibers were further translated into silica aerogel fibers (SAFs) after drying for 2 day at 80°.

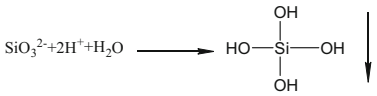

(1)

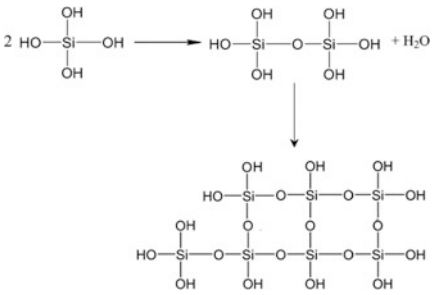

(2)

Preparation of PEDOT/SAFs. 10 mg Iron(III) p-toluene sulfonate hexahydrate dissolved in 100 mg ethanol, namely 10 wt% Iron(III) p-toluene sulfonate hexahydrate solution. And then a strand of SAFs were soaked in Iron(III) p-toluene sulfonate hexahydrate solution for 30 min. Take out SAFs and let them air-dry for 30 min. The colors of SAFs changed from colorless transparent to primrose yellow. Then put it on the copper mesh in a bottle with about 5 ml EDOT. Tighten the lid of bottle and put it in oven at 80° for 5 min. During the 5 min, EDOT) can enter the pores of SAFs, meet Iron(III) p-toluene sulfonate hexahydrate in SAFs, have polymerization and form a thin PEDOT film on the skeletons. And the colors of fibers changed from primrose yellow to black. The unreacted EDOT on fibers was washed with ethanol. In this way the PEDOT/SAFs were prepared.

Fabrication of Sensing Test Samples. 1 mm thick glass plate and PP plate were cut into uniform rectangle pieces, 2.5 cm × 1.5 cm. And a 0.5 cm × 1.5 cm small rectangle piece was removed from each PP rectangle pieces along midline of their short edge. In this way PP U-type baseplates were got. One side of PP U-type baseplates was pasted with glass rectangle piece and another side was pasted with two pieces of copper foil on the two legs of PP U-type baseplates respectively. And then a strand of PEDOT/SAFs was paste with copper foil by silver paste. In this

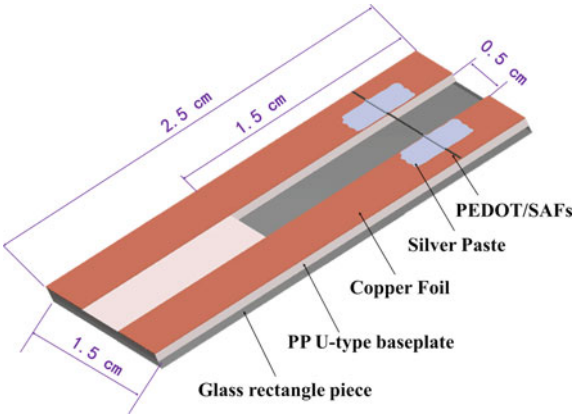

Fig. 1 Sketch of sensing test sample

Table 1 Names of SAFs and PEDOT/SAFs

Sample	Aging bath concentration (mol/L)	Loading PEDOT or not
A0.5-SAFs	0.5	Not
A0.1-SAFs	0.1	Not
A0.05-SAFs	0.05	Not
A0.01-SAFs	0.01	Not
A0-SAFs	0	Not
A0.5-PEDOT/SAFs	0.5	Loading
A0.1-PEDOT/SAFs	0.1	Loading
A0.05-PEDOT/SAFs	0.05	Loading
A0.01-PEDOT/SAFs	0.01	Loading
A0-PEDOT/SAFs	0	Loading

way the sensing test samples were fabricated. Its sketch is shown as Fig. 1. And all sample names are listed in Table 1.

Surface Area Analysis. All samples were analyzed for surface area, pore size and pore volume using N_2 adsorption–desorption isotherms (NOVATOUCH LX1, QUANTACHROME INSTRUMENTS, America). The out gas temperature was maintained at 120 °C for 5 h.

Scanning Electron Microscope. Scanning electron microscopy (SEM) images of the samples were all taken to show the morphology with SU8010, Hitachi, Japan.

Fourier-Transform Infra Red (FT-IR) Spectroscopy. Functional groups of EDOT and PEDOT were identified out using fourier-transform infra red (FT-IR) spectrometry (Spectrum BXII, Perkin Elmer, USA).

Sensing Test. The conductivity of the samples was measured using a two-point probe to show the NH_3 sensitivity of PEDOT/SAFs by Keithly 2000, USA. The environment of samples were continuously alternate between air and 1000 ppm NH_3 every 5 min. All sensing measurements were carried out at 25 °C and 60% relative humidity.

Results and Discussions

Pore Structure and Morphology of SAFs. Figure 2a is the N_2 adsorption-desorption isotherm and pore size distribution of A0.5-SAFs. As silica aerogel fibers, they have high specific surface area (760.1 m^2/g), and a lot of mesopores (average pore width is 5.29 nm). Further analysis of the results show that the adsorption isotherm does not have a plateau at high pressure ($p/p_0 > 0.9$). It is suggested that those fibers also have a number of macroporouses, and it was proven by SEM (Fig. 2d–g). The predicted macroporouses can be observed in the outside

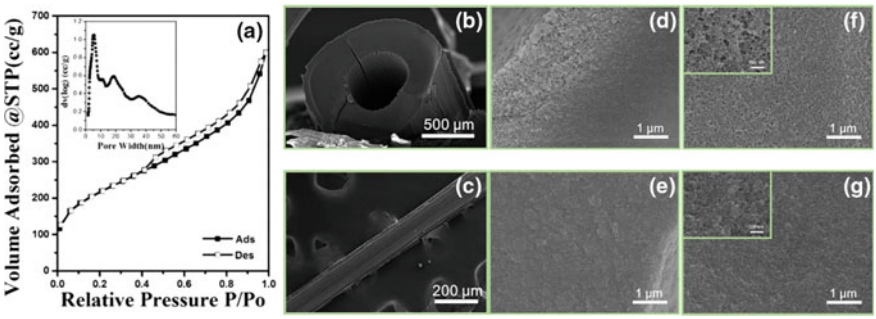

Fig. 2 **a** Nitrogen adsorption-desorption isotherms and pore-size distribution curve of A0.5-SAFs; **b**, **c** SEM images of A0.5-SAFs (hollow structure and morphology); **d**, **e** Cross-sectional images near outside surface and inside surface of A0.5-SAFs; **f**, **g** SEM images of outside surface and inside surface of A0.5-SAFs, inserts are images of partial enlargement and the scale bar is 100 nm

surfaces and inside surface. The hollow structure and uniform fiber shape can also be observed by SEM (Fig. 2b, c). Interesting that the outside surface and inside surface are loose, but the middle ring regions between outside surface and inside surface are dense. Those results indicated that the pores in surface are mainly macroporouses, the pores in he middle ring regions are mainly mesopores. Together they form a unique hierarchically macro-meso-macroporous structure.

From Fig. 2, we can find all samples have N_2 adsorption–desorption isotherms hysteretic loop and have not plateau at high pressure. Those results suggest that all samples have hierarchically macro-meso-macroporous structure. Figure 3 and Table 2 show that all samples have high specific surface area, and the specific surface area of samples prepared under high concentration coagulation bath (0.5, 0.1 and 0.05 mol/L) are much higher than under low concentration coagulation bath (0.01 and 0 mol/L). And the mesopore sizes increase first and then decrease with increase of coagulation bath concentration.

FT-IR Spectroscopy. After the polymerization from EDOT to PEDOT, the C-H which adjoined sulfur atom will disappear. Therefore, the corresponding absorption peak (about 890.9 nm^{-1}) of fourier-transform infra red spectroscopy will disappear too. And this phenomenon was observed from Fig. 4.

Sensing Test. The obtained results of sensing tests are given in Fig. 5. What's interesting is that the resistance variations of PEDOT/SAFs based on A0.01-SAFs and A0-SAFs (about 40 and 70% respectively) are much higher others. However, their specific surface area is much lower than others. This phenomenon is contrary to the reports. In order to explore the causes leading to this phenomenon, the pore structure and morphology of PEDOT/SAFs were studied too.

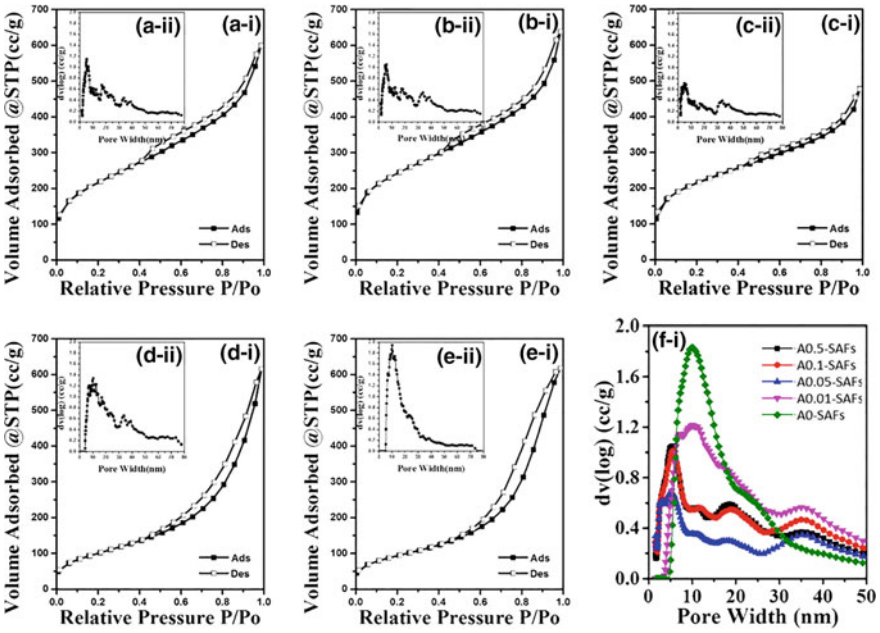

Fig. 3 Nitrogen adsorption-desorption isotherms and pore-size distribution curve of SAFs prepared using different concentrations of sulphuric acid as ageing bath. **a** A0.5- SAFs; **b** A0.1-SAFs; **c** A0.05-SAFs; **d** A0.01-SAFs; **e** A0-SAFs

Table 2 BET data of SAFs prepared using different concentrations of sulphuric acid as ageing bath

Sample	Specific surface area (m^2/g)	Pore volume (cc/g)	Pore width (nm)
A0.5-SAFs	760.1	0.93	5.29
A0.1-SAFs	835.8	0.99	5.88
A0.05-SAFs	731.6	0.74	4.89
A0.01-SAFs	364.8	0.96	10.13
A0-SAFs	333.8	0.96	10.13

Pore Structure and Morphology of PEDOT/SAFs. Firstly, the surface morphologies of PEDOT/SAFs were studied by SEM (Fig. 6). There were only a handful of macropores in the surface of all PEDOT/SAFs except A0-PEDOT/SAFs. And their macropore sizes were smaller than A0.01-PEDOT/SAFs and A0-PEDOT/SAFs.

Their N_2 adsorption-desorption isotherm and pore size distribution shown that all samples still have mesopores and macropores Fig. 7 and Table 3. But their specific surface area was much lower than corresponding SAFs. In addition, the peak heights of dv(log) were all decrease markedly. Those suggest that the pores

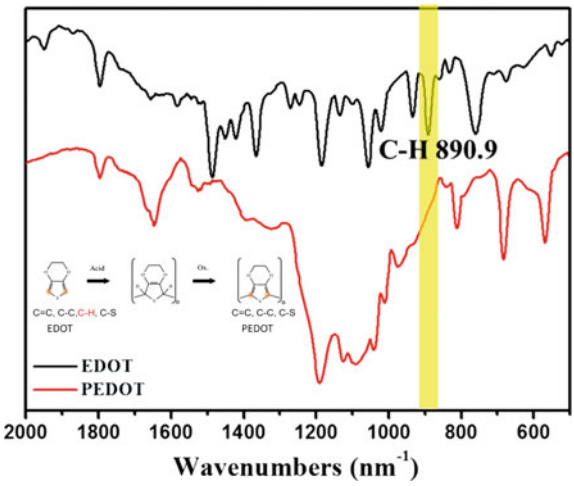

Fig. 4 FTIR spectrum of EDOT and PEDOT

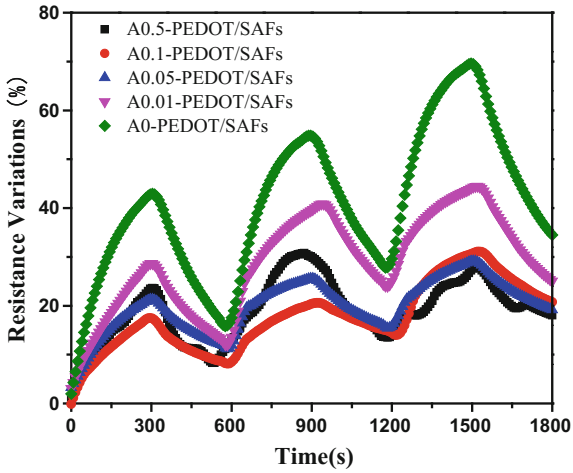

Fig. 5 Response of different PEDOT/SAFs under cyclic exposure of NH_3

narrows down and even were partly blocked by PEDOT, and this limited access for NH_3 gas. Because A0-SAFs have largest mesopore and macropore sizes, their pores have enough port area to pass NH_3 gas. Especially, there were lots of macropores retained in the surface of A0-PEDOT/SAFs. This ensures rapid entrance of NH_3 gas through macropores in the surface to mesopores in the middle ring region. Therefore, A0-PEDOT/SAFs have best gas sensitivity. Based on the analysis, we can expect the gas sensitivity should further improve, if the pore size of substrate is larger or the thickness of PEDOT is thinner. And it will be researched in our next work.

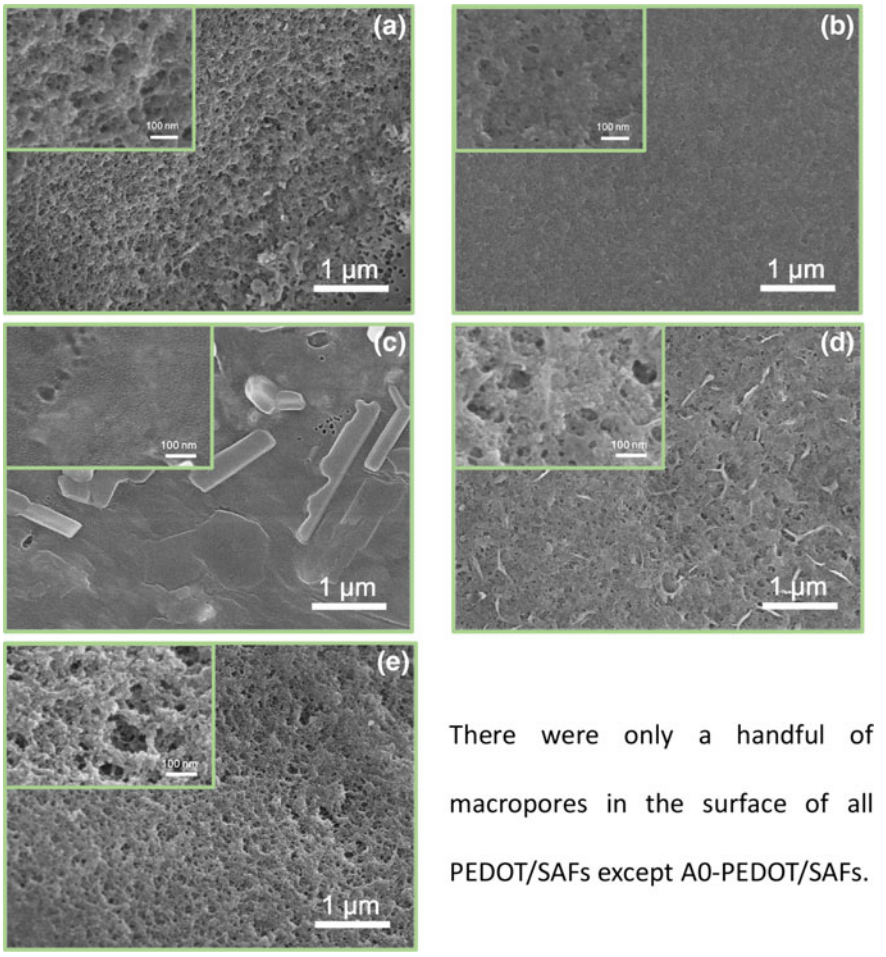

Fig. 6 SEM of surface morphologies of PEDOT/SAFs, **a** A0.5-PEDOT/SAFs; **b** A0.1-PEDOT/SAFs; **c** A0.05-PEDOT/SAFs; **d** A0.01-PEDOT/SAFs; **e** A0-PEDOT/SAFs, inserts are images of partial enlargement and the scale bar is 100 nm

Summary

In conclusion, we prepared a kind of silica aerogel fibers (SAFs) with high specific surface area (maximum one is 835.8 m^2/g), hierarchical structure and hollow structure by wet spinning. Based on SAFs, we further prepared a series of gas sensor materials, A0.5-PEDOT/SAFs, A0.1-PEDOT/SAFs, A0.05-PEDOT/SAFs, A0.01-PEDOT/SAFs and A0-PEDOT/SAFs. And A0-PEDOT/SAFs shows the best gas sensitivity. The reasons were analyzed via pore structure and morphology of PEDOT/SAFs. Finally, further improvement is put forwarded.

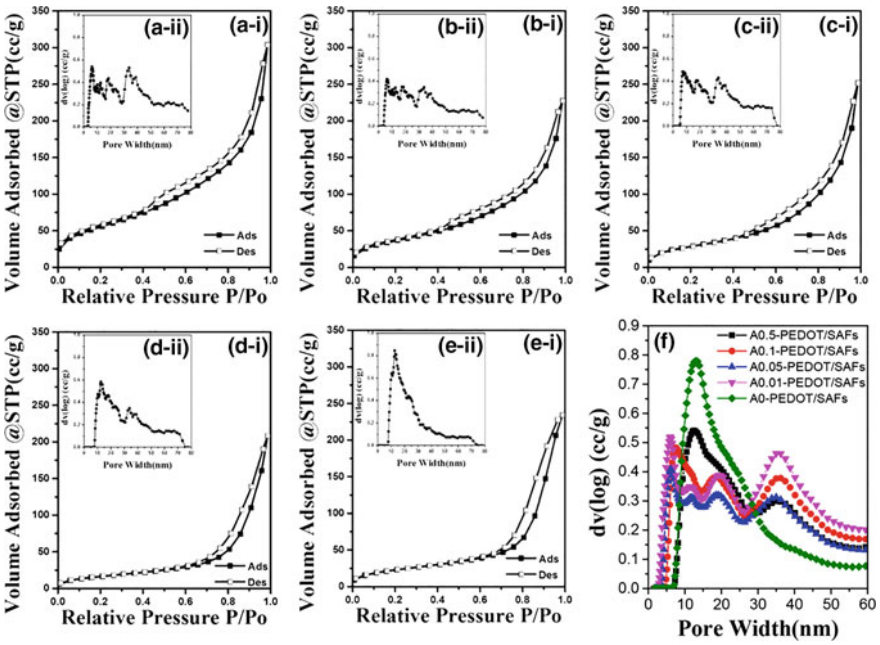

Fig. 7 Nitrogen adsorption-desorption isotherms and pore-size distribution curve of SAFs prepared using different concentrations of sulphuric acid as ageing bath. **a** A0.5-PEDOT/SAFs; **b** A0.1-PEDOT/SAFs; **c** A0.05-PEDOT/SAFs; **d** A0.01-PEDOT/SAFs; **e** A0-PEDOT/SAFs

Table 3 BET data of PEDOT/SAFs prepared using different concentrations of sulphuric acid as ageing bath

Sample	Specific surface area (m^2/g)	Pore volume (cc/g)	Pore width (nm)
A0.5-PEDOT/SAFs	199.7	0.47	5.88
A0.1-PEDOT/SAFs	132.0	0.35	5.88
A0.05-PEDOT/SAFs	105.6	0.40	6.79
A0.01-PEDOT/SAFs	60.1	0.32	12.55
A0-PEDOT/SAFs	82.8	0.36	12.55

Acknowledgements This work was supported by Shanghai Fundamental Research Projects (Project No. 16JC1400701) and Program for Changjiang Scholars and Innovative Research Team in University (IRT16R13).

References

1. J. Zhang, C. Zhang, J. Xia, Q. Li, D. Jiang, X. Zheng, Mixed-potential NH_3 sensor based on Ce0.8Gd0.2O1.9 solid electrolyte. Sens. Actuators B-Chem. **249**, 76–82 (2017)
2. A. Marutaphan, Y. Seekaew, C. Wongchoosuk, Hierarchically porous carbon derived from polymers and biomass: effect of interconnected pores on energy applications. Nanoscale Res. Lett. **12**, 90 (2017)
3. M. Eising, C.E. Cava, R.V. Salvatierra, A.J. Gorgatti Zarbin, L.S. Roman, Doping effect on self-assembled films of polyaniline and carbon nanotube applied as ammonia gas sensor. Sens. Actuators B-Chem. **245**, 25–33 (2017)
4. H. Hoang Thi, G. Ho Truong, H. Van Nguyen, T. Tran, T. Van Chu, Two-dimensional net-like SnO_2/ZnO heteronanostructures for high-performance H_2S gas sensor. Sens. Actuators B-Chem. **249**, 348–356 (2017)
5. X. Wang, S. Meng, W. Ma, J. Pionteck, M. Gnanaseelan, Z. Zhou, B. Sun, Z. Qin, M.F. Zhu, Fabrication and gas sensing behavior of poly (3, 4-ethylenedioxythiophene) coated polypropylene fiber with engineered interface. React. Funct. Polym. **112**, 74–80 (2017)
6. M. Tebyetekerwa, X. Wang, I. Marriam, P. Dan, S.Y. Yang, M.F. Zhu, Green approach to fabricate Polyindole composite nanofibers for energy and sensor applications. Mater. Lett. **209**, 400–403 (2017)
7. U. Lange, N.V. Roznyatouskaya, V.M. Mirsky, Conducting polymers in chemical sensors and arrays. Anal. Chim. Acta **614**, 1–26 (2008)
8. D. Li, J. Huang, R.B. Kaner, Polyaniline nanofibers: a unique polymer nanostructure for versatile applications. Acc. Chem. Res. **42**, 135–145 (2009)
9. S. Virji, J.X. Huang, R.B. Kaner, B.H. Weiller, Polyaniline nanofiber gas sensors: examination of response mechanisms. Nano Lett. **4**, 491–496 (2004)
10. W. Zhou, Y. Guo, H. Zhang, Y. Su, M. Liu, B. Dong, A highly sensitive ammonia sensor based on spinous core-shell PCL-PANI fibers. J. Mater. Sci. **52**, 6554–6566 (2017)
11. Z. Jing, J. Zhan, Fabrication and gas-sensing properties of porous ZnO nanoplates. Adv. Mater. **20**, 4547–4551 (2008)
12. L.E. Kreno, K. Leong, O.K. Farha, M. Allendorf, R.P. Van Duyne, J.T. Hupp, Metal-organic framework materials as chemical sensors. Chem. Rev. **112**, 1105–1125 (2012)
13. C.-J. Chang, C.-K. Lin, C.-C. Chen, C.-Y. Chen, E.-H. Kuo, Gas sensors with porous three-dimensional framework using TiO_2/polymer double-shell hollow microsphere. Thin Solid Films **520**, 1546–1553 (2011)
14. S. Dutta, A. Bhaumik, K.C.W. Wu, Hierarchically porous carbon derived from polymers and biomass: effect of interconnected pores on energy applications. Energy Environ. Sci. **7**, 3574–3592 (2014)
15. D. Fu, C. Zhu, X. Zhang, C. Li, Y. Chen, Two-dimensional net-like SnO_2/ZnO heteronanostructures for high-performance H_2S gas sensor. J. Mater. Chem. A **4**, 1390–1398 (2016)
16. E. Montes, U. Schwingenschlogl, Superior selectivity and sensitivity of blue phosphorus nanotubes in gas sensing applications. J. Mater. Chem. C **5**, 5365–5371 (2017)
17. T. Liu, J. Liu, Q. Liu, R. Li, H. Zhang, X. Jing, J. Wang, Shape-controlled fabrication and enhanced gas sensing properties of uniform sphere-like $ZnFe_2O_4$ hierarchical architectures. Sens. Actuators B-Chem. **250**, 111–120 (2017)
18. N. Wei, H. Cui, X. Wang, X. Xie, M. Wang, L. Zhang, J. Tian, Hierarchical assembly of In_2O_3 nanoparticles on ZnO hollow nanotubes using carbon fibers as templates: enhanced photocatalytic and gas-sensing properties. J. Colloid Interface Sci. **498**, 263–270 (2017)
19. B. Le Ouay, M. Boudot, T. Kitao, T. Yanagida, S. Kitagawa, T. Uemura, Nanostructuration of PEDOT in porous coordination polymers for tunable porosity and conductivity. J. Am. Chem. Soc. **138**, 10088–10091 (2016)

20. Y. Yang, S. Li, W. Yang, W. Yuan, J. Xu, Y. Jiang, In situ polymerization deposition of porous conducting polymer on reduced graphene oxide for gas sensor. ACS Appl. Mater. Interfaces **6**, 13807–13814 (2014)
21. E. Zampetti, S. Pantalei, A. Muzyczuk, A. Bearzotti, F. De Cesare, C. Spinella, A. Macagnano, A high sensitive NO_2 gas sensor based on PEDOT-PSS/TiO_2 nanofibres. Sens. Actuators B: Chem. **176**, 390–398 (2013)
22. J. Tan, M. Dun, L. Li, J. Zhao, W. Tan, Z. Lin, X. Huang, Synthesis of hollow and hollowed-out Co_3O_4 microspheres assembled by porous ultrathin nanosheets for ethanol gas sensors: responding and recovering in one second. Sens. Actuators B-Chem. **249**, 44–52 (2017)
23. W. Tan, J. Tan, L. Li, M. Dun, X. Huang, Nanosheets-assembled hollowed-out hierarchical Co_3O_4 microrods for fast response/recovery gas sensor. Sens. Actuators B-Chem. **249**, 66–75 (2017)
24. B. Winther-Jensen, O. Winther-Jensen, M. Forsyth, D.R. Macfarlane, High rates of oxygen reduction over a vapor phase-polymerized PEDOT electrode. Science **321**, 671–674 (2008)
25. B. Winther-Jensen, K. West, Vapor-phase polymerization of 3,4-ethylenedioxythiophene: a route to highly conducting polymer surface layers. Macromolecules **37**, 4538–4543 (2004)
26. B. Winther-Jensen, J. Chen, K. West, G. Wallace, Vapor phase polymerization of pyrrole and thiophene using iron(III) sulfonates as oxidizing agents. Macromolecules **37**, 5930–5935 (2004)